materials

MDPI

Article

The Study of Magnetoimpedance Effect for Magnetoelectric Laminate Composites with Different Magnetostrictive Layers

Lei Chen [1], Yao Wang [2,*], Tianhong Luo [1,*], Yongkang Zou [1,*] and Zhongjie Wan [1]

[1] Key Lab of Computer Vision and Intelligent Information System, Chongqing University of Arts and Sciences, Chongqing 402160, China; 67638515@163.com (L.C.); future_wan@foxmail.com (Z.W.)
[2] School of Electronic Information and Electrical Engineering, Shanghai Jiao Tong University, Shanghai 200240, China
* Correspondence: yaowang898@sjtu.edu.cn (Y.W.); tianhong.luo@163.com (T.L.); ycddzyk@163.com (Y.Z.)

Abstract: The rectangular magnetoelectric (ME) composites of Metglas/PZT and Terfenol-D/PZT are prepared, and the effects of a magnetostrictive layer's material characteristics on the magnetoimpedance of ME composite are discussed and experimentally investigated. The theoretical analyses show that the impedance is not only dependent on Young's modulus and the magnetostrictive strain of magnetostrictive material but is also influenced by its relative permeability. Compared with Terfenol-D, Metglas possesses significantly higher magnetic permeability and larger magnetostrictive strain at quite low H_{dc} due to the small saturation field, resulting in the larger magnetoimpedance ratio. The experimental results demonstrate that the maximum magnetoimpedance ratios (i.e., $\Delta Z/Z$) of Metglas/PZT composite are about 605.24% and 239.98% at the antiresonance and resonance, respectively. Specifically, the maximum $\Delta Z/Z$ of Metglas/PZT is 8.6 times as high as that of Terfenol-D/PZT at the antiresonance. Such results provide the fundamental guidance in the design and fabrication of novel multifunction devices based on the magnetoimpedance effect of ME composites.

Keywords: magnetostrictive material; magnetoimpedance effect; magnetostrictive strain; magnetic permeability; Young's modulus; magnetoelectric composite

Citation: Chen, L.; Wang, Y.; Luo, T.; Zou, Y.; Wan, Z. The Study of Magnetoimpedance Effect for Magnetoelectric Laminate Composites with Different Magnetostrictive Layers. *Materials* **2021**, *14*, 6397. https://doi.org/10.3390/ma14216397

Academic Editor: Christian Müller

Received: 28 September 2021
Accepted: 22 October 2021
Published: 25 October 2021

1. Introduction

The magnetoelectric (ME) laminate composites consisting of magnetostrictive and piezoelectric materials have gained intense research interests due to their applications in multifunctional devices such as memory devices, tunable inductors, magnetic sensors, electrostatically tunable filters and spin-charge transducers, etc. [1–10]. ME composites are especially promising for tunable electrical component (resistors, capacitors, inductors, etc.) applications [11–14], among which E-field tunable inductors based on ME laminate composites have been widely studied recently. Fang et al. have reported the electric-field-induced inductance change for a heterogeneous composite consisting of a PZT bar embedded in a MnZn ferrite ring [15]. Lou et al. experimentally studied the electrostatically tunable magnetoelectric inductors with multiferroic composite cores consisting of Metglas/lead zirconate titanate/Metglas [16]. Zhang et al. proposed a tunability-improved ME inductor in the symmetrical composite consisting of $Ni_{0.8}Zn_{0.2}Fe_2O_4$ platelet and piezoelectric ceramics $Pb(Zr,Ti)O_3$ slab with laminate Metglas foils [17]. Additionally, DC magnetic field (H_{dc}) tuning of electrical components has attracted much attention and become an exciting research topic. Singh et al. investigated the giant magnetocapacitance of magnetoelectric $Bi_{0.5}Na_{0.5}TiO_3/NiFe_2O_4$ composite at a high magnetic field [18]. Zhang et al. studied the effect of boundary conditions on the magnetocapacitance of a ring-type magnetoelectric structure [19]. Wang et al. have also reported the large room-temperature magnetocapacitance in the $Tb_xDy_{1-x}Fe_{2-y}/PbZr_xTi_{1-x}O_3/Tb_xDy_{1-x}Fe_{2-y}$ laminate at a saturated magnetic field of 1.5 kOe [13].

The magnetically tunable capacitance, inductance and impedance effects provide a promising application for sensors and transducers, etc. However, few articles have discussed tuning the giant magnetoimpedance (MI) effect of ME composites with the DC magnetic field at room temperature [20,21]. Additionally, compared to the conventional magnetoelectric (ME) effect, the MI effect of ME composite can be obtained by applying only the DC magnetic field (H_{dc}) without superimposing the alternating magnetic field (H_{ac}), which decreases the power consumption and facilitates the miniaturization of the ME device. Furthermore, the analysis and comparisons of various magnetostrictive material's influences on the MI effect of ME composites are rarely reported, which hinders the design and optimization of tunable magnetoimpedance devices. Correspondingly, to facilitate the practical device applications, it is both physically interesting and technologically important to study and understand the magnetoimpedance effect of ME composites with different magnetostrictive materials.

In this work, the magnetoimpedance (MI) effects of ME laminate composites with different magnetostrictive materials are analyzed and experimentally investigated. It is interesting to find that the Metglas/PZT laminate composite demonstrates the significantly higher MI effect compared to Terfenol-D/PZT laminate composite, whose maximum impedance ratio is 8.6 times as high as that of Terfenol-D/PZT at the antiresonance frequency. Furthermore, the influences of different magnetostrictive materials (e.g., Metglas and Terfenol-D) on the MI effect of ME composites are analyzed and corresponding resonant frequencies are explored. It is interesting to find that the effective magnetic permeability, magnetostrictive strain and Young's modulus of magnetostrictive materials play critical roles in improving the magnetoimpedance effect of ME composites.

2. Experiment

The rectangular Metglas/PZT and Terfenol-D/PZT bilayer composites were prepared to investigate the magnetoimpedance effect of ME composite. The PZT plate with dimensions of $12 \times 6 \times 0.8$ mm^3 was supplied by Electronics Technology Group Corporation No.26 Research Institute, Chongqing, China, which exhibits the high ferroelectric Curie temperature and piezoelectric constant. The Ag electrodes of PZT were distributed on the top and bottom surfaces, and the PZT was polarized with an electric field of 25 kV/cm along the thickness direction. Terfenol-D with giant saturation magnetostriction (~1200 ppm) was purchased from Gansu Tianxing Rare Earth Functional Materials Co., Ltd., Gansu, China. Then the Terfenol-D layer was cut into a rectangular plate with a length of 12 mm, width of 6 mm and thickness of 1 mm. The soft magnetostrictive Metglas 2605SA1 (i.e., FeBSiC) with extremely high relative permeability (μ_r = 50,000) and good mechanical properties was produced by Foshan Huaxin Microlite Metal Co., Ltd., Foshan, China, and the size is $12 \times 6 \times 0.03$ mm^3. To fabricate the ME samples, the Terfenol-D plates were dipped into acetone to clean the surface oxidation layer at first. Then, the piezoelectric layer and magnetostrictive layer were bonded together with epoxy adhesive, which were pressed using a hydraulic press and cured at 80 °C for 4 h to minimize the epoxy thickness between layers.

The external DC magnetic field (H_{dc}) was generated by a pair of annular permanent magnets (Nd–Fe–B), which is along the longitudinal direction of the ME composite. The H_{dc} between 0 and 1500 Oe was calibrated by a Gaussmeter. Then the impedance of ME composites was measured with a precision impedance analyzer (4194 A HP Agilent, Santa Clara, CA, USA), as shown in Figure 1. Specifically, the impedance spectrum was measured at different DC magnetic fields by using a frequency-swept method around the resonance frequency. It is noted that before the impedance measurements, the standard calibration was performed under open and short circuit conditions to eliminate the inherent features of the measured system associated with the connecting cable and background circuit. Furthermore, magnetization hysteresis (M–H) and strain coefficients were measured with the vibrating sample magnetometer (VSM) and laser Doppler vibrometer (Polytec OFV-5000, Berlin, Germany), respectively.

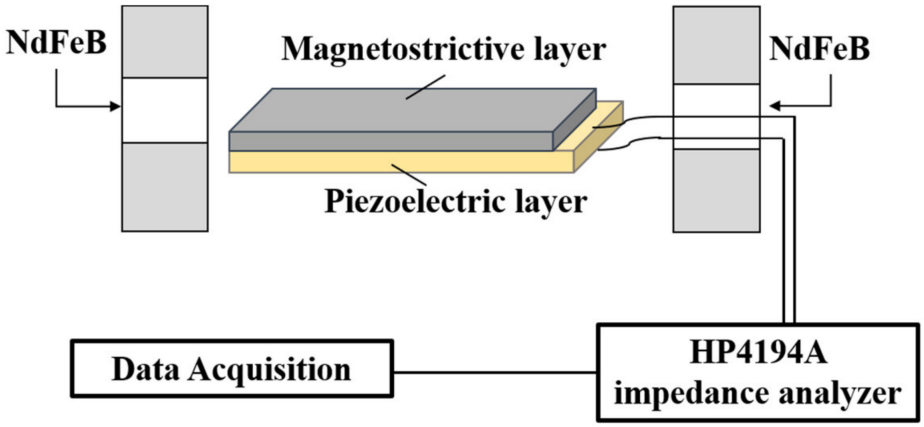

Figure 1. Schematic diagram of the dynamic measurement setup for investigating the MI effect of ME composite.

3. Results and Discussion

To investigate the magnetoimpedance of ME composites, the impedance of Metglas/PZT composite was measured as a function of electrical excitation frequency under different longitudinal DC magnetic fields, as shown in Figure 2. It is interesting to find that both the antiresonance frequency f_a corresponding to the maximum impedance (Z_m) and the resonance frequency f_r corresponding to the minimum impedance (Z_n) show strong dependences on H_{dc}, shown as the insets of Figure 3. f_r and f_a vary with the DC magnetic field in a similar trend for the ME composite. For Metglas/PZT composite, f_r and f_a increase quickly with the increased DC magnetic field until the magnetization of Metglas reaches saturation. The resonance frequency f_r varies from 138.3 to 139.3 kHz when H_{dc} increases from 0 Oe to 600 Oe. Such changes of f_r and f_a are attributed to the ΔE effects of magnetostrictive material as a function of the DC magnetic field. Specifically, the Young's modulus E_m of magnetostrictive material varies with DC magnetic field due to the different magnetic domain movements under various magnetic fields. Since the resonance frequency of the ME composite is proportional to the square root of the ME composite's average Young's modulus $\overline{E}$ ($\overline{E} = n_p E_p + n_m E_m$, n_p and n_m are the volume fraction of piezoelectric and magnetostrictive materials, respectively) [22], the resonance frequency shifts with the increased DC magnetic field accordingly.

It is also shown in Figure 3 that the maximum impedance (Z_m) and minimum impedance (Z_n) vary nonmonotonically with the DC magnetic field. It is found that for Metglas/PZT composite, Z_m increases sharply until reaching a peak at H_{dc} = 40 Oe, then it gradually reaches a stable value with the further increased H_{dc}. The variations of maximum and minimum impedances for both ME composites are due to both factors: on the one hand, when a DC magnetic field is applied along the length direction of the ME composite, the magnetostrictive material elongates and shrinks in the plane due to the piezomagnetic effect and ΔE effect. Then such magnetostrictive strain and stress transfer to the neighboring piezoelectric material due to the interface coupling, which lead to the varied dielectric polarization of ME composite with increasing H_{dc}. On the other hand, the relative permeability of magnetostrictive material decreases with the increased DC magnetic field along the length direction since the large H_{dc} plays a damping role on the magnetic domain movement. In this case, the strong dependence of Z on the effective relative permeability μ_{eff} and dielectric polarization ε_{eff} lead to the change of Z with the DC magnetic field. The detailed analysis is as follows.

According to the report by Salahun et al. [23], the impedance of ME laminate composite can be determined by Equation (1), as

$$Z = \sqrt{\frac{\mu_0 \mu_{eff}}{\varepsilon_0 \varepsilon_{eff}}} \quad (1)$$

where μ_0 and μ_{eff} are vacuum permeability and relative effective permeability of magnetostrictive material, respectively. ε_0 and ε_{eff} are vacuum permittivity and relative effective permittivity of piezoelectric material, respectively. At low electrical excitation frequencies, the thickness of magnetostrictive material is far less than the skin depth, and the thickness of the piezoelectric material is far less than the sound wavelength in the material.

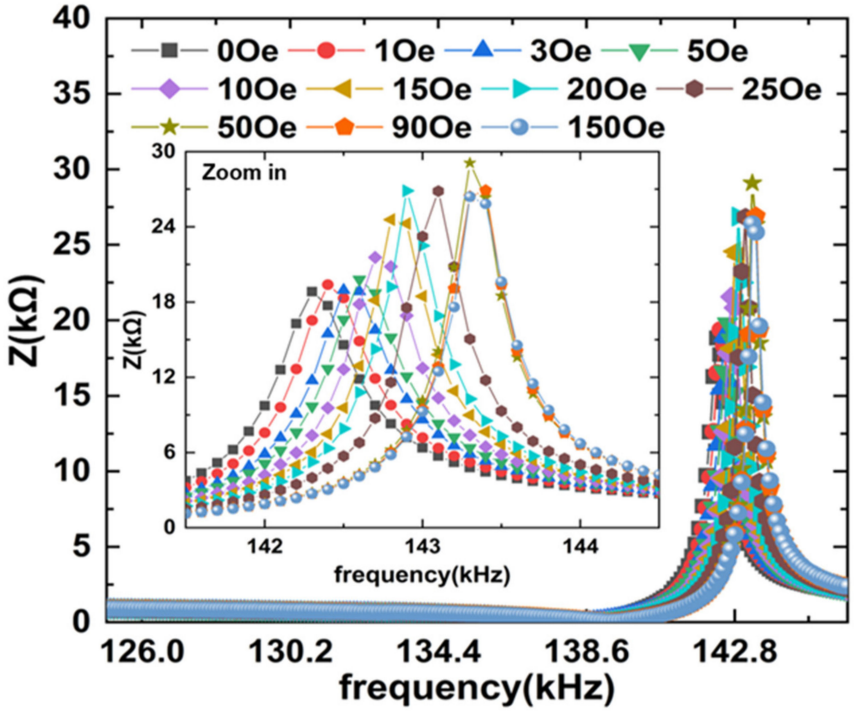

Figure 2. Impedance spectra of the bilayer Metglas/PZT composites at various DC magnetic fields. The inset shows the enlarged view near the antiresonance frequency.

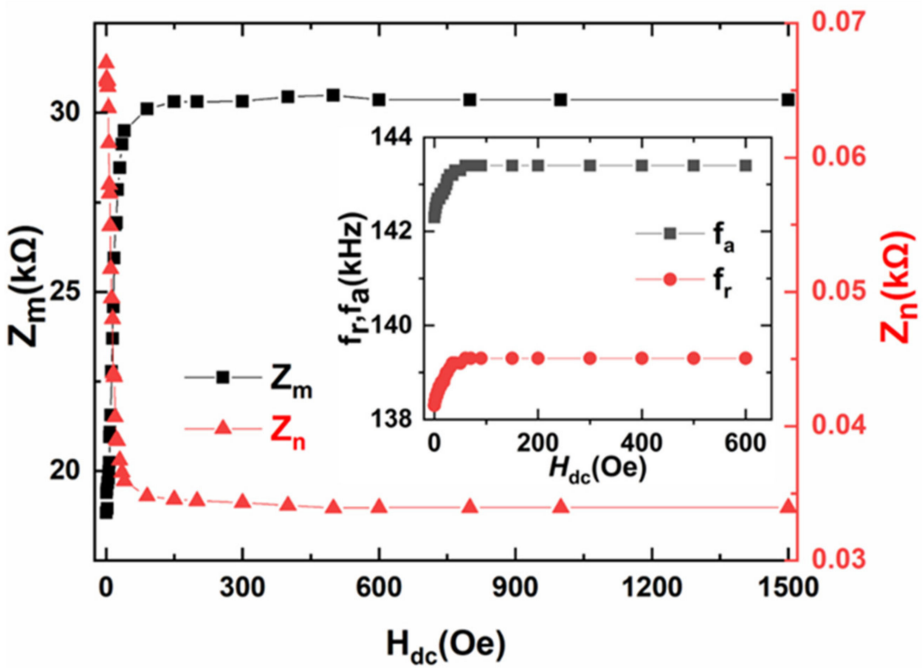

Figure 3. The minimum impedance Z_n (@the resonance frequency f_r) and maximum impedance Z_m (@the antiresonance frequency f_a) as a function of the DC magnetic field H_{dc} for bilayer Metglas/PZT composites. The inset shows the dependence of f_r and f_a on H_{dc}.

For ME laminate composite, μ_{eff} and ε_{eff} can be calculated using Wiener's law [24] as

$$\mu_{eff} = n_m(\mu_r - 1) + 1 \tag{2}$$

$$\varepsilon_{eff} = \varepsilon_r / n_p \tag{3}$$

where μ_r and ε_r are relative permeability of magnetostrictive material and relative permittivity of piezoelectric material, respectively. n_m and n_p are volume fractions of magnetostrictive and piezoelectric materials, respectively. Hence the relative permeability and permittivity of ME composite play key roles in tuning the impedance, according to Equations (1)–(3).

On the one hand, since the relative magnetic permeability of magnetostrictive material can be estimated as $\mu_r = 4\pi M_s / H_{dc} + 1$, thus the magnetic permeability varies with the applied DC magnetic field H_{dc}. From Equations (1) and (2), the strong dependence of effective relative permeability μ_{eff} on H_{dc} results in the dependence of magnetoimpedance on H_{dc}.

On the other hand, the relative permittivity varies with the change of applied mechanical stress T according to Devonshire's law [25],

$$\frac{1}{\varepsilon_r} = \frac{1}{\varepsilon_r(T = 0)} - 4Q_{12}T \tag{4}$$

where Q_{12} is the electrostriction coefficient and T is the stress. When a DC magnetic field is applied, the magnetostriction of magnetostrictive material gives rise to the mechanical stress T, which transfers to the piezoelectric material due to the stress–strain coupling of the interlayer and further leads to varied dielectric polarizations of piezoelectric material. According to the report by Srinivasan et al. in [26], the corresponding mechanical stress T of the magnetostrictive layer can be expressed as following:

$$T = \frac{E_p E_m t_m \Delta s}{(1 - \nu)(t_p E_p + t_m E_m)} \tag{5}$$

where $\nu = 0.34$ is Poisson's ratio, Δs is the magnetostrictive strain of the magnetostrictive material. E_p and E_m are the Young's modulus of piezoelectric and magnetostrictive material, respectively. t_p and t_m are the thickness of piezoelectric and magnetostrictive materials, respectively.

Substituting Equation (5) into Equation (4) yields

$$\frac{1}{\varepsilon_r} = \frac{1}{\varepsilon_r(T = 0)} - \frac{4Q_{12}E_p E_m t_m \Delta s}{(1 - \nu)(t_p E_p + t_m E_m)} \tag{6}$$

From Equation (5), it is found that the mechanical stress T resulted from the magnetostrictive material varies with the DC magnetic field H_{dc} due to the dependence of the magnetostrictive strain Δs and Young's modulus E_m on H_{dc}. Correspondingly, this leads to the change of ε_r and impedance Z with the DC magnetic field according to Equations (1) and (6).

Then by inserting Equations (2) and (3) and Equation (6) into Equation (1), the ME composite's impedance can be expressed as

$$Z = \sqrt{\mu_0 n_p \frac{n_m(\mu_r - 1) + 1}{\varepsilon_0} \left[\frac{1}{\varepsilon_r(T = 0)} - \frac{4Q_{12}E_p E_m t_m \Delta s}{(1 - \nu)(t_p E_p + t_m E_m)} \right]} \tag{7}$$

According to Equation (7), it is known that the variation of ME composite's impedance (Z) with the magnetic field H_{dc} is not only determined by the relative magnetic permeability μ_r of the magnetostrictive material but is also affected by the magnetostrictive strain Δs and Young's modulus E_m of the magnetostrictive material since the magnetostrictive stress

transferred to neighboring piezoelectric layer causes the varied ε_r. Hence, it is interesting to find that the magnetic permeability, magnetostrictive strain and Young's modulus of the magnetostrictive layer play crucial roles in improving the magnetoimpedance effect of the ME composite. Here, it is noted that the mechanism of the MI effect in ME composites differs from the giant magnetoimpedance effect in soft magnetic materials [27]. The former is determined by both the permeability and permittivity of the ME composite, while the latter is mainly affected by the skin effect and magneto-inductance of soft magnetic material.

To further validate the theoretical analysis of magnetostrictive material properties' impact on the magnetoimpedance effect, the normalized magnetization curves of Terfenol-D and Metglas were measured with the vibration sample magnetometer (VSM). Here, the DC magnetic field was applied along the longitudinal direction of the sample when the magnetization curves (Figure 4) were measured. The magnetization curve of Terfenol-D shows clear hysteretic behaviors compared with Metglas. The magnetization of Metglas reaches the saturation quickly with the increased H_{dc}, while the magnetization of Terfenol-D varies more slowly with increasing H_{dc}. This originates from the different structures of magnetic domains for Terfenol-D and Metglas, respectively. Nanosized striped domains in Metglas can be easily aligned along the direction of the applied DC magnetic field due to its small coercive field H_c and high reversibility. However, Terfenol-D possesses a larger coercive field relative to Metglas, which requires the larger DC magnetic field to reach the new magnetization state once the magnetic domains are reoriented and this leads to the hysteresis of the magnetization curve. Additionally, it is found that the maximum magnetic permeability, saturation magnetization and saturation magnetic field of Metglas are 50,000, 1016 emu cm^{-3} and 105 Oe, respectively. For comparison, the maximum magnetic permeability, saturation magnetization and saturation field of Terfenol-D are 10, 629 emu cm^{-3} and 3100 Oe, respectively. Here, the relative magnetic permeability μ_r of Metglas is 5000 times larger than that of Terfenol-D, which results in a significantly lower saturation field and produces higher magnetostrictive strain at low H_{dc} for Metglas.

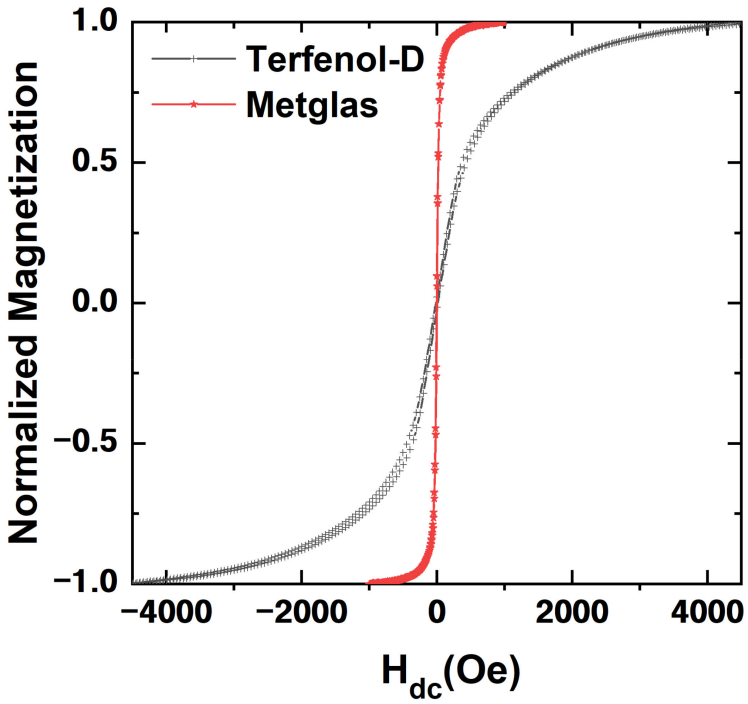

Figure 4. The measured magnetic hysteresis loops of the Metglas and Terfenol-D, respectively.

It is well known that the Young's modulus E of magnetostrictive material varies with applied DC magnetic field, i.e., ΔE effect ($\Delta E/E_0 = (E_H - E_0)/E_0$, E_H and E_0 are the elastic modulus in specific magnetic field H_{dc} and H_{dc} = 0 Oe, respectively [28,29].

Here, the variations of the elastic modulus E for the Metglas and Terfenol-D with a bias magnetic field are shown in Figure 5. For Terfenol-D, the elastic modulus E decreases slowly with increasing H_{dc} (negative-ΔE), which is mainly attributed to non-180° domain-wall motion. When H_{dc} increases to 373 Oe, the non-180° domain-wall motion achieves its maximum, and the compliance related to increased deformation is maximized, resulting in a minimum stiffness for Terfenol-D. Correspondingly, E reaches a minimum value. Then the elastic modulus E increases with further increasing H_{dc} (positive-ΔE) because the constraint of non-180° domain-wall motion at higher magnetic field tends to stiffen Terfenol-D. For comparison, the elastic modulus E of Metglas first decreases with the increased bias field and reaches a minimum value at a bias field of 3.5 Oe and the maximum negative ΔE effect occurs, then increases again until the magnetization of Metglas reaches the saturation and the positive ΔE effect happens. Hence, the dependence of Young's modulus on H_{dc} results from the varied magnetic domain movement under changing H_{dc}. It is noted that the maximum absolute value $(\Delta E/E_0)_{max}$ of Metglas is ~17.5% at low magnetic field H_{dc}, which is about two times larger than that of Terfenol-D. This is mainly attributed to the high saturation magnetic field of Terfenol-D. It is known that the ΔE effect is related to saturation magnetostriction and the saturation magnetization of the magnetic material, which can be expressed as [30]

$$\frac{\Delta E}{E_0} = \frac{9\mu_0 E_H \lambda_s^2}{20\pi M_s^2} \quad (8)$$

where μ_0 is the vacuum permeability, λ_s is the saturation magnetostriction, and M_s is the saturation magnetization. $\Delta E/E_0$ is not only determined by λ_s but is also affected by M_s. Hence, Terfenol-D with giant saturation magnetostriction will exhibit the large ΔE effect. However, such a large ΔE effect can be achieved only at the extremely high magnetic field due to the high saturation magnetization and magnetocrystalline anisotropy of Terfenol-D. Clark et al. reported that the largest $\Delta E/E_0$ effect for Terfenol-D reaches 161% at the high DC bias magnetic field of 4.3 kOe [30].

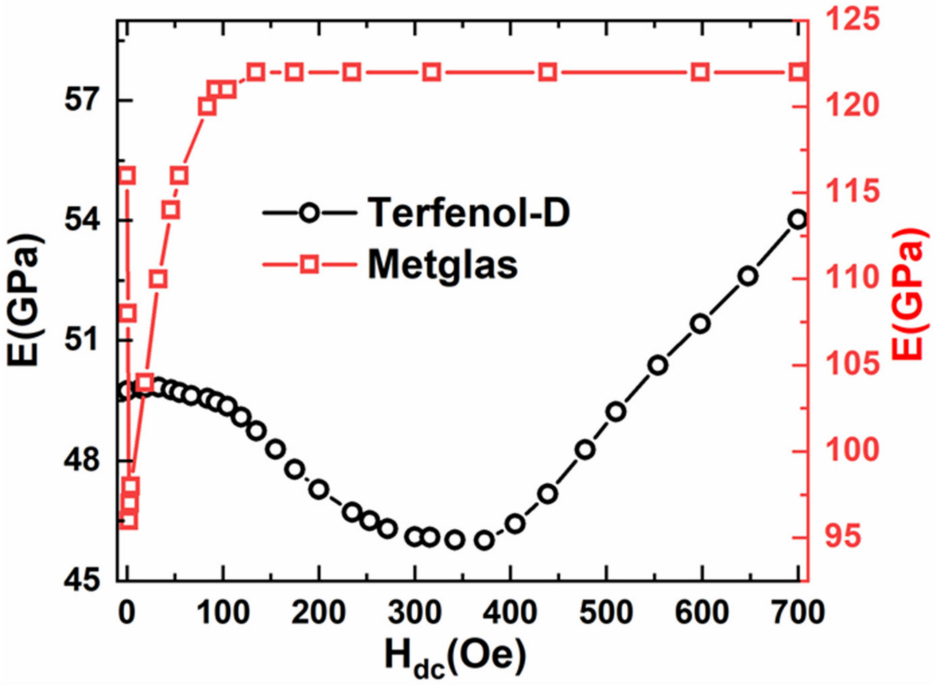

Figure 5. The elastic modulus E as a function of H_{dc} for the Metglas and Terfenol-D.

Additionally, the magnetostrictive strain coefficients d_{33} of Terfenol-D and Metglas at various H_{dc} are measured with a Laser Doppler Vibrometer LDV system, respectively, as shown in Figure 6. For the Terfenol-D, d_{33} enhances slowly and reaches a maximum value when H_{dc} increases to 373 Oe and then reduces subsequently with the further

increased H_{dc}. For the Metglas, d_{33} increases linearly with increasing H_{dc} until reaching a maximum value at H_{dc} = 3.5 Oe, and then drops rapidly to a near-zero value when H_{dc} further increases. It is interesting to find that the maximum d_{33} (Figure 6) occurs at the same H_{dc}, where the maximum negative ΔE effect (Figure 5) also happens. It indicates that the magnetostrictive materials are driven in the "burst region" of the quasi-static strain-field curve where non-180° domain-wall motion is maximum. Furthermore, it is found that the effective magnetostrictive strain coefficient d_{33} of Metglas is greater than that of Terfenol-D in a small DC magnetic bias range of $0 < H_{dc} < 33$ Oe. Specifically, the maximum value d_{33} of Metglas is about 1.2 times larger than that of Terfenol-D due to the small saturation field. This is because the magnetostrictive strain coefficient d_{33} is directly proportional to the saturation magnetostriction λ_s and the squared magnetic relative permeability μ_r [31–33]. Although the saturation magnetostriction of Terfenol-D (λ_s = 1200 ppm) is larger than that of Metglas (λ_s = 20 ppm), Terfenol-D presents a quite low relative magnetic permeability (μ_r = 10), and correspondingly, the high permeability of Metglas causes its large magnetostrictive strain coefficient at the lower DC magnetic biases.

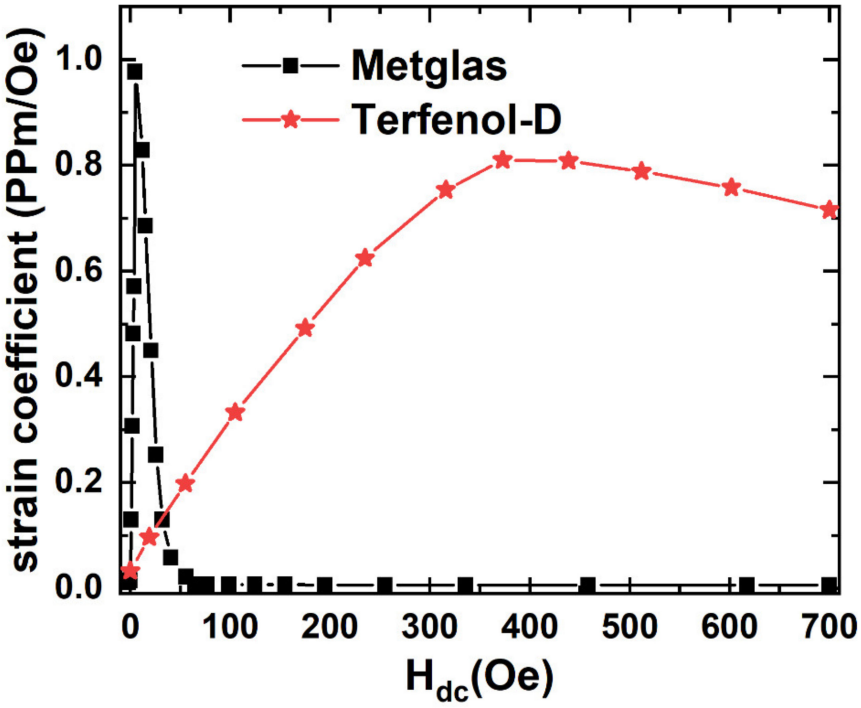

Figure 6. The strain coefficients as a function of H_{dc} for the Metglas and Terfenol-D.

It is known that the impedance of ME composite is determined by the effective magnetic permeability, Young's modulus and magnetostrictive strain of magnetostrictive material, shown as Equation (7). Correspondingly, much higher permeability, larger magnetostrictive strain, stronger ΔE effect and smaller saturation magnetic field of Metglas result in larger magnetoimpedance ratios (i.e., ΔZ/Z) for Metglas/PZT composite compared to Terfenol-D/PZT.

The magnetoimpedance ratio (MR) is defined as Equation (9) to characterize the MR effect [27,34]

$$\frac{\Delta Z}{Z} = \frac{Z(H_{dc}) - Z_{min}}{Z_{min}} \quad (9)$$

where $Z(H_{dc})$ denotes the impedance of ME composite at H_{dc} and Z_{min} denotes the minimum impedance.

For comparison, we measure impedance spectra, the minimum impedance Z_n and maximum impedance Z_m as a function of the DC magnetic field H_{dc} for Terfenol-D/PZT composite, as shown in Figure 7. For Terfenol-D/PZT composite, Z_m decreases rapidly with

the increased H_{dc} until reaching the minimum value near H_{dc} = 300 Oe, then Z_m increases again with further increased H_{dc}. Then, the MRs at the resonance f_r and antiresonance f_a are measured as a function of H_{dc} for Terfenol-D/PZT and Metglas/PZT composites, respectively, shown as Figure 8. It is found that the maximum $\Delta Z/Z$ of Terfenol-D/PZT composite is about 69.84% and 43.98% at the antiresonance frequency f_a and resonance frequency f_r, respectively. For comparison, the maximum magnetoimpedance ratios $\Delta Z/Z$ of Metglas/PZT composite are about 605.24% and 239.98% at the antiresonance and resonance frequencies, respectively. Compared with the Terfenol-D/PZT composite, the MRs of Metglas/PZT composite are much higher at both the resonance and antiresonance frequencies, respectively. For example, the maximum $\Delta Z/Z$ of Metglas/PZT composite is 8.6 times as high as that of Terfenol-D/PZT at the antiresonance frequency. The reason is as follows: although Metglas exhibits much smaller saturation magnetostriction compared to Terfenol-D, the extremely high permeability of Metglas (μ_r = 50,000) concentrates the external magnetic flux effectively and results in the high effective strain coefficient and ΔE effect in a low magnetic field, shown as Figures 5 and 6. Such strong magnetostrictive strain and ΔE effect at the low H_{dc} cause the sharply varied effective dielectric permittivity of the neighboring piezoelectric layer through the stress–strain coupling. Additionally, the relative magnetic permeability of Metglas decreases more sharply with the increased DC magnetic field due to the low saturation field. Correspondingly, a larger magnetoimpedance ratio is obtained for the Metglas/PZT composite due to the drastic change of permeability and permittivity. In contrast, even though Terfenol-D possesses a huge saturation magnetostriction (λ_s = 1200 ppm) and low Young's modulus, the low relative permeability of Terfenol-D means that a significantly higher magnetic bias field is needed to generate the large magnetostrictive strain and ΔE effect, resulting in the small variation of effective dielectric permittivity at the low bias field. Furthermore, the magnetic permeability of Terfenol-D varies more slowly with the bias magnetic field compared to Metglas. Hence, this leads to a smaller magnetoimpedance ratio of Terfenol-D/PZT composite relative to Metglas/PZT composite.

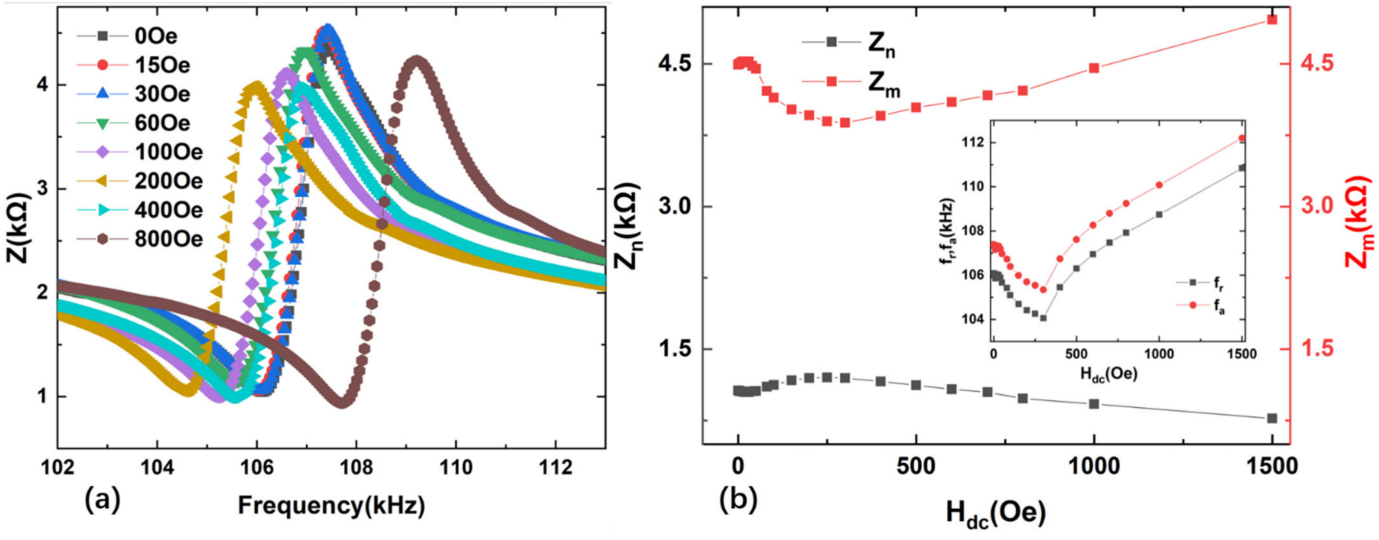

Figure 7. (**a**) Impedance spectra of the Terfenol-D/PZT composites at various DC magnetic fields. (**b**) The minimum impedance Z_n and maximum impedance Z_m as a function of the DC magnetic field H_{dc} for Terfenol-D/PZT composites. The inset shows the dependence of f_r and f_a on H_{dc}.

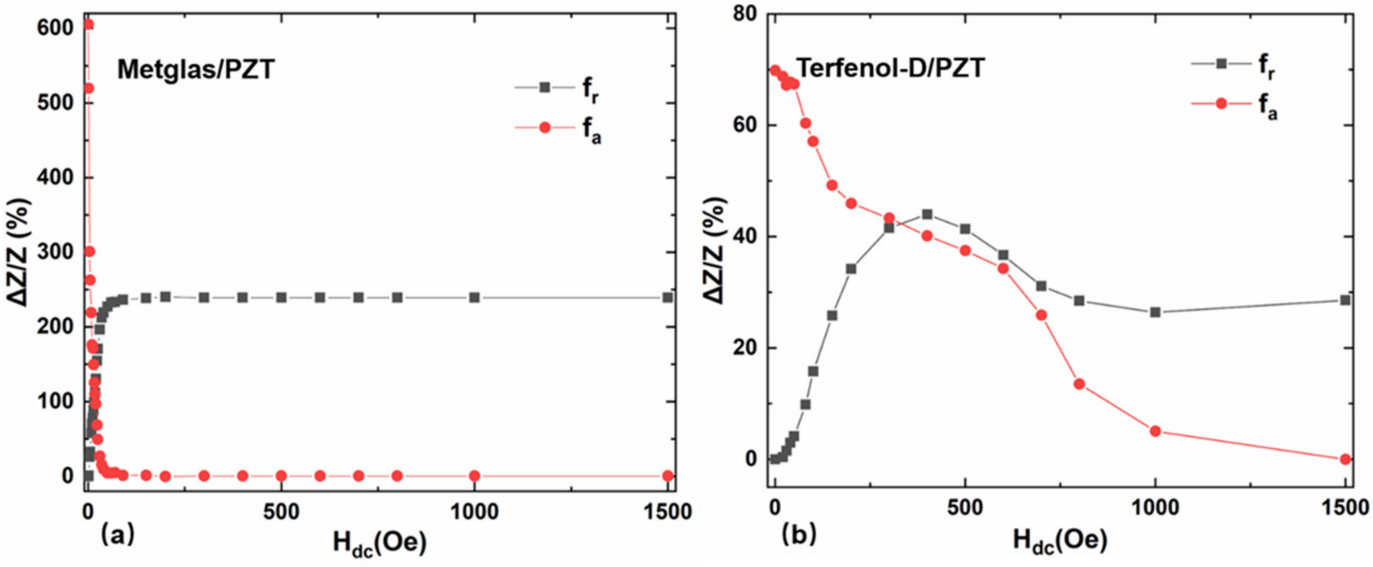

Figure 8. The magnetoimpedance ratios as a function of the DC magnetic field for (**a**) Metglas/PZT and (**b**) Terfenol-D/PZT composites at f_r and f_a, respectively.

4. Conclusions

In this study, the magnetoimpedance effects are investigated for bilayer ME composites with different magnetostrictive materials (i.e., soft magnetic amorphous ribbon Metglas and giant magnetostrictive material Terfenol-D). Both the theoretical analysis and experimental studies show that the magnetic permeability, magnetostrictive strain and Young's modulus of the magnetostrictive layer play a crucial role in the magnetoimpedance effect of ME composite. Although Metglas possesses a lower saturation magnetostriction relative to Terfenol-D, the magnetic permeability of Metglas is significantly larger than that of Terfenol-D. This leads to the larger variation of effective magnetostrictive strain at the low bias field and corresponding larger MI effect. The experimental results show that the maximum magnetoimpedance ratio of Metglas/PZT composite is about 605.24% at the antiresonance frequency, which is 8.6 times as high as that of Terfenol-D/PZT. The study indicates that the magnetoimpedance effect can be improved significantly by utilizing the magnetostrictive material with optimum material properties, which provides guidance for designing a magnetically tunable electrical device.

Author Contributions: Conceptualization, Y.W.; data curation, L.C., T.L., Y.Z. and Z.W.; formal analysis, T.L., Y.Z. and Z.W.; funding acquisition, L.C. and T.L.; investigation, L.C., Y.W., T.L., Y.Z. and Z.W.; project administration, L.C.; resources, Z.W.; writing—original draft, L.C. and Y.W.; writing—review and editing, Y.W. and Y.Z. All authors have read and agreed to the published version of the manuscript.

Funding: This research is supported by the National Natural Science Foundation of China (Grant No. 61304255), the Scientific and Technological Research Program of Chongqing Municipal Education Commission (No. KJZD-K201901301), the Natural Science Foundation of Chongqing (No. cstc2020jcyj-msxmX0899), and key projects of technological innovation and application demonstration in Chongqing (Grant No. cstc2018jszx-cyzdX0175).

Institutional Review Board Statement: Not applicable.

Informed Consent Statement: Not applicable.

Data Availability Statement: Data sharing is not applicable to this article.

Conflicts of Interest: The authors declare no conflict of interest.

References

1. Leung, C.M.; Zhuang, X.; Gao, M.; Tang, X.; Xu, J.; Li, J.; Zhang, J.; Srinivasan, G.; Viehland, D. Enhanced stability of magnetoelectric gyrators under high power conditions. *Appl. Phys. Lett.* **2017**, *111*, 182901. [CrossRef]
2. Zhang, R.; Zhang, S.; Xu, Y.; Zhou, L.; Liu, F.; Xu, X. Modeling of a magnetoelectric laminate ring using generalized hamilton's principle. *Materials* **2019**, *12*, 1442. [CrossRef]
3. Zhang, J.; Kang, Y.; Gao, Y.; Weng, G.J. Experimental investigation of the magnetoelectric effect in NdFeB-driven a-line shape terfenol-D/PZT-5A structures. *Materials* **2019**, *12*, 1055. [CrossRef] [PubMed]
4. Chu, Z.; Pourhosseiniasl, M.J.; Dong, S. Review of multi-layered magnetoelectric composite materials and devices applications. *J. Phys. D Appl. Phys.* **2018**, *51*, 243001. [CrossRef]
5. Rupp, T.; Truong, B.D.; Williams, S.; Roundy, S. Magnetoelectric transducer designs for use as wireless power receivers in wearable and implantable applications. *Materials* **2019**, *12*, 512. [CrossRef] [PubMed]
6. Chen, L.; Wang, Y. The effects of the soft magnetic alloys' material characteristics on resonant magnetoelectric coupling for magnetostrictive/piezoelectric composites. *Smart Mater. Struct.* **2019**, *28*, 045003. [CrossRef]
7. Zhuang, X.; Leung, C.M.; Sreenivasulu, G.; Gao, M.; Zhang, J.; Srinivasan, G.; Li, J.; Viehland, D. Upper limit for power conversion in magnetoelectric gyrators. *Appl. Phys. Lett.* **2017**, *111*, 163902. [CrossRef]
8. Hu, J.-M.; Duan, C.-G.; Nan, C.-W.; Chen, L.-Q. Understanding and designing magnetoelectric heterostructures guided by computation: Progresses, remaining questions, and perspectives. *NPJ Comput. Mater.* **2017**, *3*, 1–21. [CrossRef]
9. Spetzler, B.; Kirchhof, C.; Reermann, J.; Durdaut, P.; Höft, M.; Schmidt, G.; Quandt, E.; Faupel, F. Influence of the quality factor on the signal to noise ratio of magnetoelectric sensors based on the delta-E effect. *Appl. Phys. Lett.* **2019**, *114*, 183504. [CrossRef]
10. Li, M.; Matyushov, A.; Dong, C.; Chen, H.; Lin, H.; Nan, T.; Qian, Z.; Rinaldi, M.; Lin, Y.; Sun, N.X. Ultra-sensitive NEMS magnetoelectric sensor for picotesla DC magnetic field detection. *Appl. Phys. Lett.* **2017**, *110*, 143510. [CrossRef]
11. Liu, G.; Cui, X.; Dong, S. A tunable ring-type magnetoelectric inductor. *J. Appl. Phys.* **2010**, *108*, 094106. [CrossRef]
12. Yan, Y.; Geng, L.D.; Zhang, L.; Tu, C.; Sriramdas, R.; Liu, H.; Li, X.; Sanghadasa, M.; Ngo, K.D.T.; Wang, Y.U.; et al. High-Power Magnetoelectric Voltage Tunable Inductors. *IEEE Trans. Ind. Electron.* **2021**, *68*, 5355–5365. [CrossRef]
13. Wang, W.; Luo, X.B.; Zhang, N.; Ma, Q.Y. Giant room-temperature magnetocapacitance in Terfenol-D/PZT/Terfenol-D trilayer composites. *Sens. Actuator. A Phys.* **2011**, *171*, 248–251. [CrossRef]
14. Zhang, J.J.; Wen, J.B.; Gao, Y.W. A nonlinear model for magnetocapacitance effect in PZT-ring/Terfenol-D-strip magnetoelectric composites. *AIP Adv.* **2016**, *6*, 065318. [CrossRef]
15. Fang, X.; Zhang, N.; Wang, Z.L. Converse magnetoelectric effects on heterotype electrostrain-piezopermeability composites. *Appl. Phys. Lett.* **2008**, *93*, 102503. [CrossRef]
16. Lou, J.; Reed, D.; Liu, M.; Sun, N.X. Electrostatically tunable magnetoelectric inductors with large inductance tunability. *Appl. Phys. Lett.* **2009**, *94*, 112508. [CrossRef]
17. Zhang, J.; Chen, D.; Filippov, D.A.; Zhang, Q.; Li, K.; Hang, X.; Ge, B.; Cao, L.; Srinivasan, G. Improved tunability in Metglas/Ferrite/PZT magnetoelectric tunable inductors. *IEEE Trans. Magn.* **2019**, *55*, 1–4. [CrossRef]
18. Singh, P.; Laishram, R.; Sharma, P.; Kolte, J. Giant magnetocapacitance in magnetoelectric BNT/NFO particulate composites. *J. Mater. Sci. Mater. Electron.* **2021**, *32*, 21288–21296. [CrossRef]
19. Zhang, J.J. Effect of boundary conditions on magnetocapacitance effect in a ring-type magnetoelectric structure. *Phys. Lett. A* **2017**, *381*, 3909–3916. [CrossRef]
20. Leung, C.M.; Zhuang, X.; Xu, J.; Li, J.; Zhang, J.; Srinivasan, G.; Viehland, D. Enhanced tunability of magneto-impedance and magneto-capacitance in annealed Metglas/PZT magnetoelectric composites. *AIP Adv.* **2018**, *8*, 055803. [CrossRef]
21. Wang, W.; Wang, Z.; Luo, X.; Tao, J.; Zhang, N.; Xu, X.; Zhou, L. Capacitive type magnetoimpedance effect in piezoelectric-magnetostrictive composite resonator. *Appl. Phys. Lett.* **2015**, *107*, 172904. [CrossRef]
22. Wan, J.G.; Li, Z.Y.; Wang, Y.; Zeng, M.; Wang, G.H.; Liu, J.M. Strong flexural resonant magnetoelectric effect in Terfenol-D/epoxy-Pb(Zr,Ti)O_3 bilayer. *Appl. Phys. Lett.* **2005**, *86*, 202504. [CrossRef]
23. Salahun, E.; Queffelec, P.; Tanne, G.; Adenot, A.-L.; Acher, O. Correlation between magnetic properties of layered ferromagnetic/dielectric materials and tunable device applications. *J. Appl. Phys.* **2002**, *91*, 5449–5455. [CrossRef]
24. Born, M.; Wolf, E. *Principle of Optics*; Pergamon Press: New York, NY, USA, 1959; p. 803.
25. Suo, Z. Stress and strain in ferroelectrics. *Curr. Opin. Solid State Mater. Sci.* **1998**, *3*, 486–489. [CrossRef]
26. Bichurin, M.I.; Petrov, V.M.; Srinivasan, G. Theory of low-frequency magnetoelectric coupling in magnetostrictive-piezoelectric bilayers. *Phys. Rev. B* **2003**, *68*, 054402. [CrossRef]
27. Yang, Z.; Lei, C.; Zhou, Y.; Sun, X. Study of the giant magnetoimpedance effect in micro-patterned co-based amorphous ribbons with single strip structure sand tortuous shape. *Microsyst. Technol.* **2015**, *21*, 1995. [CrossRef]
28. Engdahl, G. *Handbook of Giant Magnetostrictive Materials*; Academic Press: San Diego, CA, USA, 2000.
29. Or, S.W.; Nersessian, N.; Carman, G.P. Dynamic magnetomechanical behavior of Terfenol-D/Epoxy 1–3 particulate composites. *IEEE Trans. Magn.* **2004**, *40*, 71–77. [CrossRef]
30. Clark, A.E.; Savage, H.T. Giant magnetically induced changes in the elastic moduli in $Tb_{.3}Dy_{.7}Fe_2$. *IEEE Trans. Sonics Ultrason.* **1975**, *22*, 50. [CrossRef]
31. Cullity, B.D. *Introduction to Magnetic Materials*; Addison-Wesley Press: Cambridge, MA, USA, 1972.

32. Xing, Z.P.; Zhai, J.Y.; Dong, S.X.; Li, J.F.; Viehland, D.; Odendaal, W.G. Modeling and detection of quasi-static nanotesla magnetic field variations using magnetoelectric laminate sensors. *Meas. Sci. Technol.* **2008**, *19*, 015206. [CrossRef]
33. Chen, L.; Li, P.; Wen, Y.; Qiu, J. The magnetostrictive material effects on magnetic field sensitivity for magnetoelectric sensor. *J. Appl. Phys.* **2012**, *111*, 07E503. [CrossRef]
34. Wang, Y.; Wen, Y.; Song, F.; Li, P.; Yu, S. Enhanced inductance in laminated multilayer magnetic planar inductor for sensitive magnetic field detection. *Appl. Phys. Lett.* **2018**, *112*, 182403. [CrossRef]